AD-A039 861 AIL DEER PARK N Y F/G 4/1
IHR (INFRARED HETERODYNE RADIOMETER) FOR LOW ALTITUDE TEMPERATU--ETC(U)
APR 77 I RUBINSTEIN N00014-76-C-0721
UNCLASSIFIED AIL-C618-1 NL

1 OF 1
AD A039 861

END

DATE FILMED
6-77

IHR FOR LOW ALTITUDE TEMPERATURE PROFILE RETRIEVAL

ANNUAL REPORT

by

I. RUBINSTEIN

AIL REPORT NO. C618-1

APRIL 1977

PREPARED UNDER CONTRACT N00014-76-C-0721
OFFICE OF NAVAL RESEARCH
WASHINGTON, D.C.

AIL a division of CUTLER-HAMMER
DEER PARK, LONG ISLAND, NEW YORK 11729

IHR FOR LOW ALTITUDE TEMPERATURE PROFILE RETRIEVAL

ANNUAL REPORT

by

I. RUBINSTEIN

AIL REPORT NO. C618-1

APRIL 1977

PREPARED UNDER CONTRACT N00014-76-C-0721

OFFICE OF NAVAL RESEARCH

WASHINGTON, D.C.

TASK NUMBER NR211-203/4-01-77 (465)

AIL a division of CUTLER-HAMMER

DEER PARK, LONG ISLAND, NEW YORK 11729

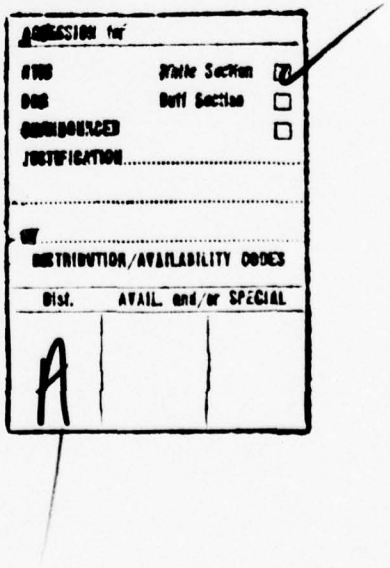

Unclassified

SECURITY CLASSIFICATION OF THIS PAGE (When Data Entered)

(14) AIL-C618-1

REPORT DOCUMENTATION PAGE

READ INSTRUCTIONS BEFORE COMPLETING FORM

1. REPORT NUMBER: C618-1
2. GOVT ACCESSION NO.
3. RECIPIENT'S CATALOG NUMBER

(6) 4. TITLE (and Subtitle): IHR (Infrared Heterodyne Radiometer) for Low Altitude Temperature Profile Retrieval.

(9) 5. TYPE OF REPORT & PERIOD COVERED: Annual rept., Apr[redacted]76-Apr[redacted]77

6. PERFORMING ORG. REPORT NUMBER

7. AUTHOR(s)

(10) I. Rubinstein

8. CONTRACT OR GRANT NUMBER(s)

(15) N00014-76-C-0721 new

PERFORMING ORGANIZATION NAME AND ADDRESS

AIL, a division of Cutler-Hammer
Deer Park, New York 11729

10. PROGRAM ELEMENT, PROJECT, TASK AREA & WORK UNIT NUMBERS

11. CONTROLLING OFFICE NAME AND ADDRESS

Office of Naval Research
800 N. Quincy Street
Arlington, Virginia 22217

(11) 12. REPORT DATE: Apr[redacted]77

13. NUMBER OF PAGES

(12) 37p.

14. MONITORING AGENCY NAME & ADDRESS (if different from Controlling Office)

15. SECURITY CLASS. (of this report)

Unclassified

15a. DECLASSIFICATION/DOWNGRADING SCHEDULE

16. DISTRIBUTION STATEMENT (of this Report)

Approved for public release; distribution unlimited

17. DISTRIBUTION STATEMENT (of the abstract entered in Block 20, if different from Report)

18. SUPPLEMENTARY NOTES

19. KEY WORDS (Continue on reverse side if necessary and identify by block number)

Infrared - Radiometer, Temperature - Retrieval
Index of Refraction Variation

20. ABSTRACT (Continue on reverse side if necessary and identify by block number)

A technique for obtaining accurate temperature and humidity profiles with a grazing-angle up-looking radiometer has been investigated. The profiling technique is based on information retrievals which are obtained from difference-kernel functions generated from pairs of high spectral resolution radiometric channels. Spatially selective information can be generated from such functions with the required accuracy for → next page

DD FORM 1 JAN 73 1473 EDITION OF 1 NOV 65 IS OBSOLETE

Unclassified

SECURITY CLASSIFICATION OF THIS PAGE (When Data Entered)

ONR 404967

ABSTRACT (continued)

retrieving temperature gradients at the lower altitude atmospheric levels.

A retrieval of an assumed double inverted temperature profile in the lower atmosphere, using three differential kernel information channels of CO_2 signature emission in the 13 μm region, has been simulated. The retrieval is based on iterative solutions of the radiative transfer equation and requires no apriori statistical knowledge of the atmospheric temperature profile. Temperature inversions at 375 and 750 meters, assumed for the selected atmospheric model, were reproduced in the simulated retrieval. However, the retrieved profile lacked detail at the immediate altitude above ground level due to the excessive spatial widths of the difference-kernel functions.

TABLE OF CONTENTS

LIST OF ILLUSTRATIONS

I. INTRODUCTION

This program is aimed at the development of radiometric techniques for the remote measurement of atmospheric temperature and humidity profiles. The generated profiles are expected to be instrumental in the assessment of apparent errors in target positions resulting from refraction index gradients along an atmospheric propagation path.

Remote altitude profile measurements of temperature and concentrations of gas constituents in the atmosphere have been previously implemented by radiometric measurement of the up-welling radiance using aircraft, satellite, and balloon platforms. (References 1, 2 and 3). Unfortunately the altitude resolution obtainable with up-looking radiometers using similar techniques is inherently poor due to the erratic response of kernel functions associated with down-welling radiation. Therefore, the measured information for an up-looking radiometer lacks sufficient detail to retrieve properties of the lower atmosphere where sharper gradients of temperature and humidity often occur as a function of diurnal and other atmospheric conditions.

An alternate technique for obtaining more accurate temperature and humidity profiles with a grazing-angle up-looking radiometer has been investigated. The profiling technique is based on information retrievals which are obtained from difference-kernel functions generated from pairs of high spectral resolution radiometric channels. Spatially selective information can be generated from such functions with the required accuracy for retrieving temperature gradients at the lower altitude atmospheric levels.

A retrieval of an assumed double inverted temperature profile in the lower atmosphere, using three differential kernel information channels of CO_2 signature emission in the 13 μm region, has been simulated. The retrieval is based on iterative solutions of the radiative transfer equation and requires no apriori statistical knowledge of the atmospheric temperature profile. Temperature inversions at 375 and 750 meters, assumed for the selected atmospheric model, were reproduced in the simulated retrieval. However, the retrieved profile lacked detail at the immediate altitude above ground level due to the excessive spatial widths of the difference-kernel functions.

A four information channel retrieval, based on higher selective functions, will be investigated during the next phase of this program.

II. GENERAL SCOPE

In general, variations in the atmospheric refraction index may be classified as:

- Small-scale
- Large-scale

Small scale variations are associated with clear air turbulence phenomena in the lower atmosphere and are manifested in random fluctuations of amplitude and phase of energy transferred through the medium, with a time constant in the millisecond range. The large scale refraction index profile; of interest in this study, is a relatively long time property of an atmospheric path which is a function of average values of local pressure, temperature and humidity along the path.

The refractive index n of the atmosphere is conveniently described in terms of the refractivity N, in parts per millions, by the expression,

$$n = 1 + 10^{-6} N$$
$$\text{or } N = (n-1)\, 10^{6} \qquad (1)$$

The refractivity at optical wavelengths is related to local temperature and pressure (Reference 4) by:

$$N \approx 79 \frac{P}{T} \qquad (2)$$

where: P = pressure in millibars

T = temperature in degrees kelvin

The downward bending curvatuve of an optical ray at a given altitude level is given by the gradient of the refractivity:

$$C = \frac{dN}{dh} = - \frac{79}{T} \frac{dP}{dh} + \frac{79P}{T^2} \frac{dT}{dh} \qquad (3)$$

For radio and microwave frequency propagation, an additional term due to humidity gradient enters into the above curvature equation.

Absolute values of local temperature and pressure as a function of altitude entering in equation (3), may be estimated within a small error from reported statistical data for given geographic area and measured ground (or ocean) temperature. Similarly, close estimates on pressure vs altitude gradients are obtained from universal curves. The situation however is quite different for the case of temperature gradients. Available statistical data on temperature profiles provide good estimates on gradients at relatively high altitudes. At the lower altitudes however, changes in the gradient

directions (i.e., inversions) occur frequently as a result of many atmospheric variables, (e.g., position of the sun, overcase condition, surface and ambient temperature, wind velocity and direction), which result in substantial error in assessing the true target position.

Measured temperature gradients at lower altitude using radiosonde techniques are given in Figure 1. The double inversion in the gradient (superadiabatic) is typical for mid-day condition whereby the surface temperature is higher than the surrounding ambient temperature. Positive inversion at ground level (not shown in Figure 1), on the other hand typically occurs at night. The neutral gradient (Figure 1) is normally typical for early morning and later afternoon conditions. It is clear that the uncertainty in the changing gradient and associated inversions in vicinity of ground or ocean surface is the largest source of potential error in estimating the local curvatures in ray bending for grazing-angle uplooking pointing or direction finding detection systems.

This study is aimed at establishing the feasibility of determining the temperature and humidity gradient profiles at the lower altitude levels by means of remote radiometric measurements. Using this measurement information in conjunction with statistical/measured data on local atmospheric conditions (temperature, pressure and humidity), assessing target error positions in real time appears to be feasible.

III. BASIC PHENOMENOLOGY IN RADIOMETRIC PROFILING

The average apparent radiance sensed by a radiometer viewing the atmosphere is governed by the steady-state atmospheric radiation transfer equation as illustrated schematically in Figure 2.

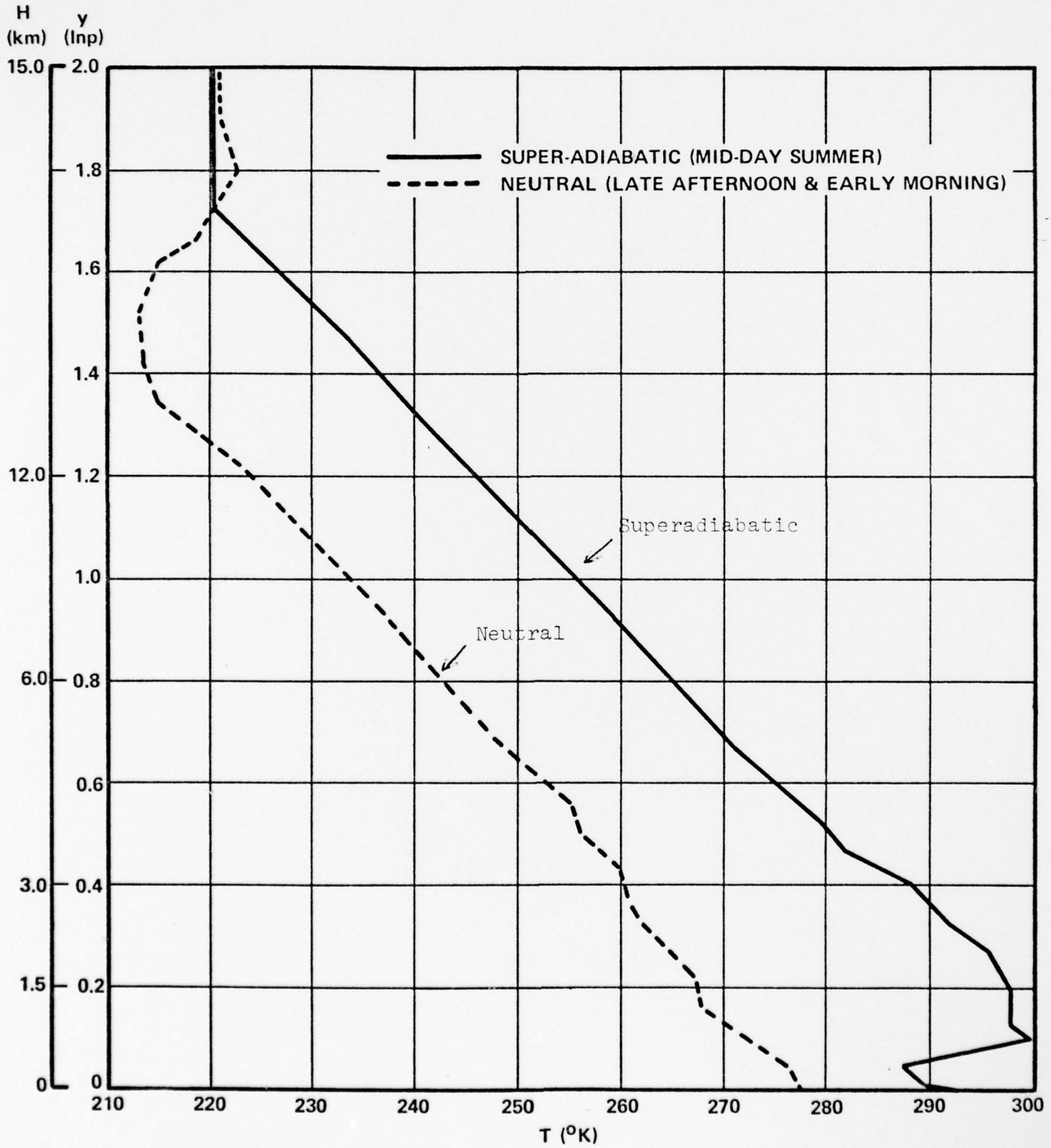

Figure 1. Radiosonde Measured Temperature Profiles

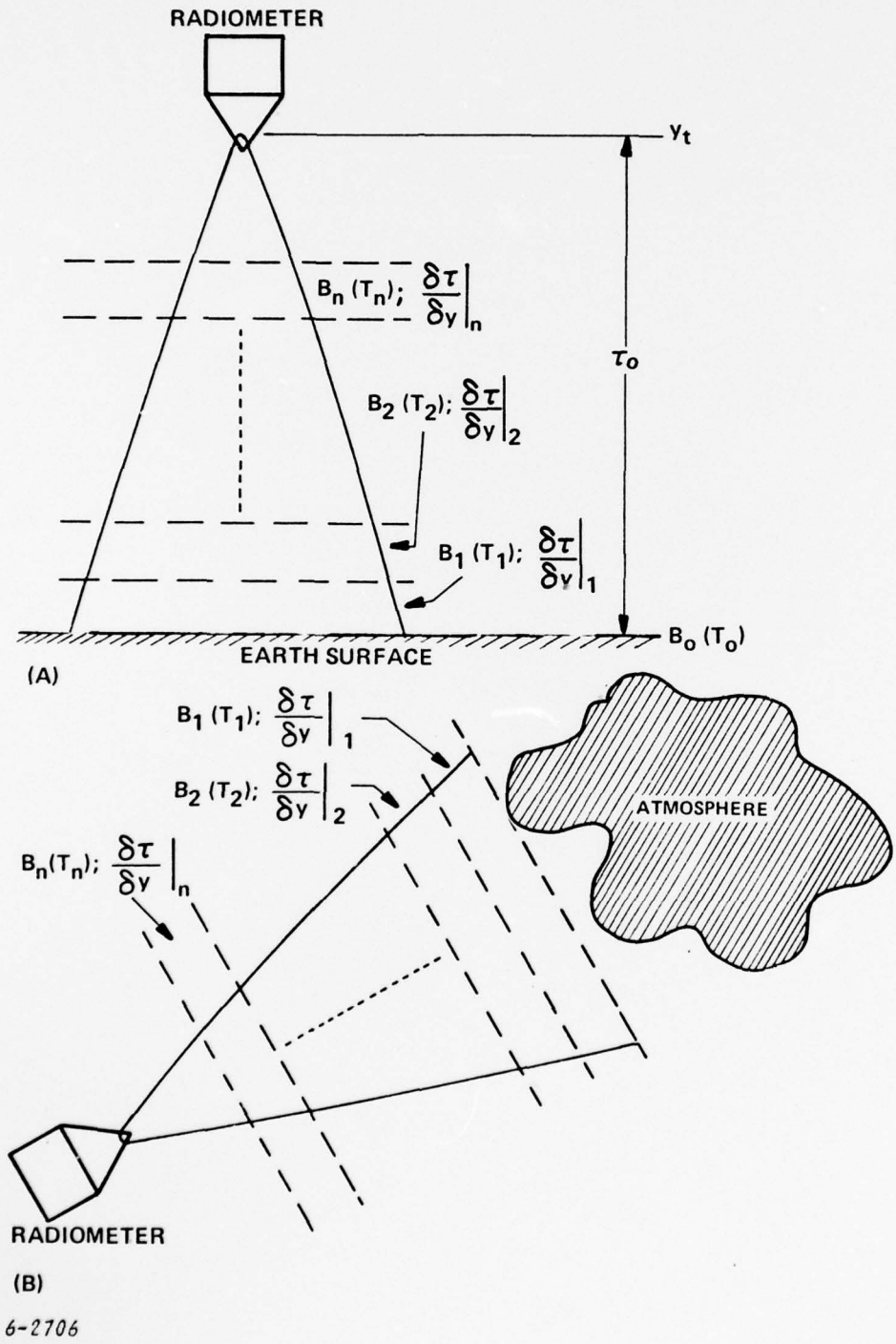

Figure 2. Steady-State Atmospheric Radiation Transfer

For a down-looking radiometer (Figure 2A), the apparent radiance is given by:

$$N_A = B_o(T)\ \tau_o + \int_o^{y_t} B_i(T)\ \frac{\partial \tau_i}{\partial y}\ dy \qquad (4)$$

where:

B_o, B_i = Planck's radiances at ground and ith altitude-level, respectively

τ_o, τ_i = atmospheric transmission coefficients in the total propagation path from ground level to receiver, and ith altitude level to receiver, respectively

y = normalized spatial coordinate

The first term in the right-hand side of equation (4) is due to the earth (or ocean) radiance as attenuated in its total propagation path. The second term represents re-emission of radiance in the various atmospheric layers within the total propagation path.

A similar transfer equation may be obtained for an up-looking radiometric system (Figure 2B).

$$N_A = \int_{y_t}^{o} B_i(T)\ \frac{\partial \tau_i}{\partial y}\ dy \qquad (5)$$

where the sensed radiance is due to atmospheric emission only.

One method of radiometric profiling consists of implementing several spectral sensor-channels, each selectively accepting emitted radiation from limited spatial regions. Such an ideal up-looking profile radiometric system is depicted in Figure 3. As shown, it consists of a multitude of sensor channels, each having rectangular

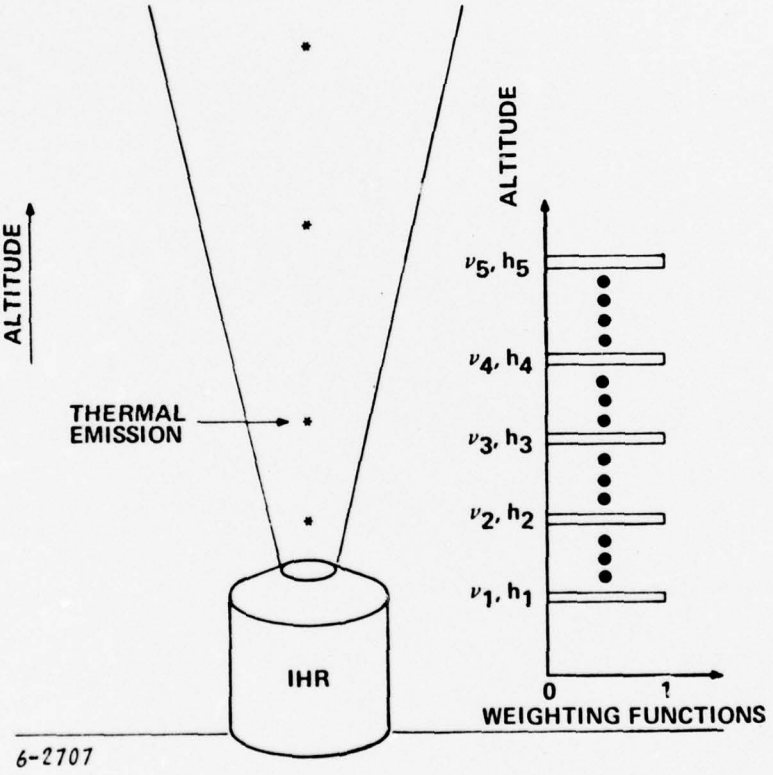

Figure 3. Ideal Profiling - Radiometer Concept

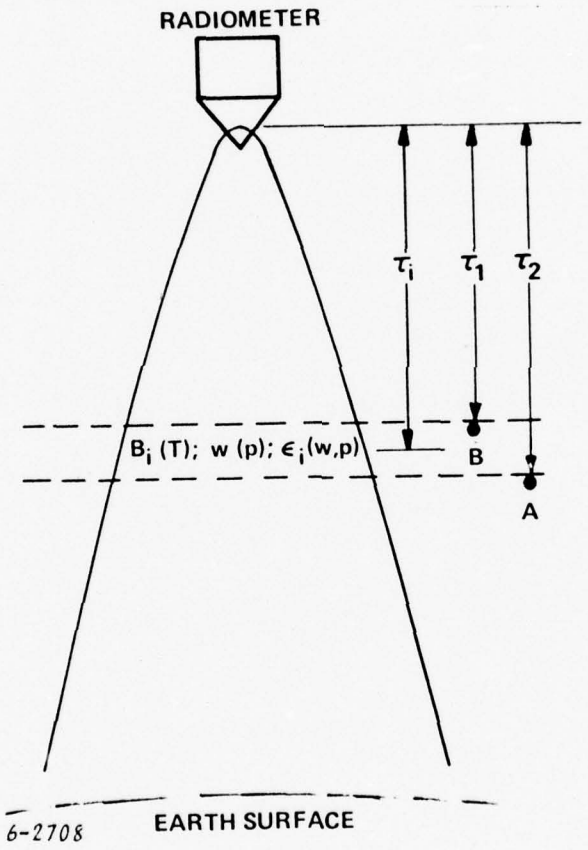

Figure 4. Sensible Radiance from Single Atmospheric Layer

narrow response characteristics sensitive to radiation from discrete altitude levels. In practice, the responses of the channels are broadened by natural characteristics in the signature profiles of the emitting gases as well as by their relative distribution with altitude levels. Since the response widths of the actual channel are finite, they must be contiguous so as to encompass the total profiled range of interest.

The basic parameters associated with radiometric profiling are defined in Figure 4, where a down-looking radiometer is viewing an "atmospheric layer" within its field-of-view. The pertinent radiometric parameters are:

$B_i(T)$ = Planck's radiance

$W_i(p)$ = concentration of active gas

$\epsilon(W,p)$ = gas emissivity

T = temperature

p = pressure

It should be noted that though gas concentration and emissivity are also functions of temperature, this functional dependency is small as compared to that due to pressure, and hence, it is neglected here. The apparent radiance emanating from the layer as sensed by the radiometer is shown in Figure 4 and given by:

$$N_i = B_i(T) \quad \epsilon_i \tau_i \qquad (6)$$

where τ_i is the transmission coefficient of the total path from ith level to receiver.

The apparent emission relationship in equation (6) may be expressed in a somewhat alternate form. Referring to Figure 4, assume a radiance source $B_s(T)$ alternately located at points A and B, below and above the atmospheric layer considered, respectively. The apparent absorption within the layer is then given by:

$$N_{ABS} = B_s(T) \left[\tau_1 - \tau_2\right] \tag{7}$$

From Kirchof's law of absorption-emission equivalency, the coefficient in equation (6) is equivalent to the transmissivity difference in equation (7) which may also be expressed in a differential form, namely:

$$_i\tau_i = \tau_1 - \tau_2 = \frac{\partial \tau_i}{\partial y} dy \tag{8}$$

The spatial derivatives $\frac{\partial \tau_i}{\partial y}$, referred to as kernels or weighting functions, are the linear coefficient of the temperature dependent Planck's radiance in equations (4) and (5). Hence, the spatial selectivity of a radiometer is determined from response characteristics of the kernels as a function of altitude.

The difference in the nature of response of the kernels for up-looking and down-looking systems may be visualized by referring to Figure 5. For a down-looking radiometer (Figure 5A), the concentration in the active gas and hence the emissivity is decreasing along the direction of radiation. The transmission coefficient increaases along the direction of the propagation path. Hence, peaking of the weighting function along the propagation path will occur. For an up-looking radiometer, no peaking will occur since

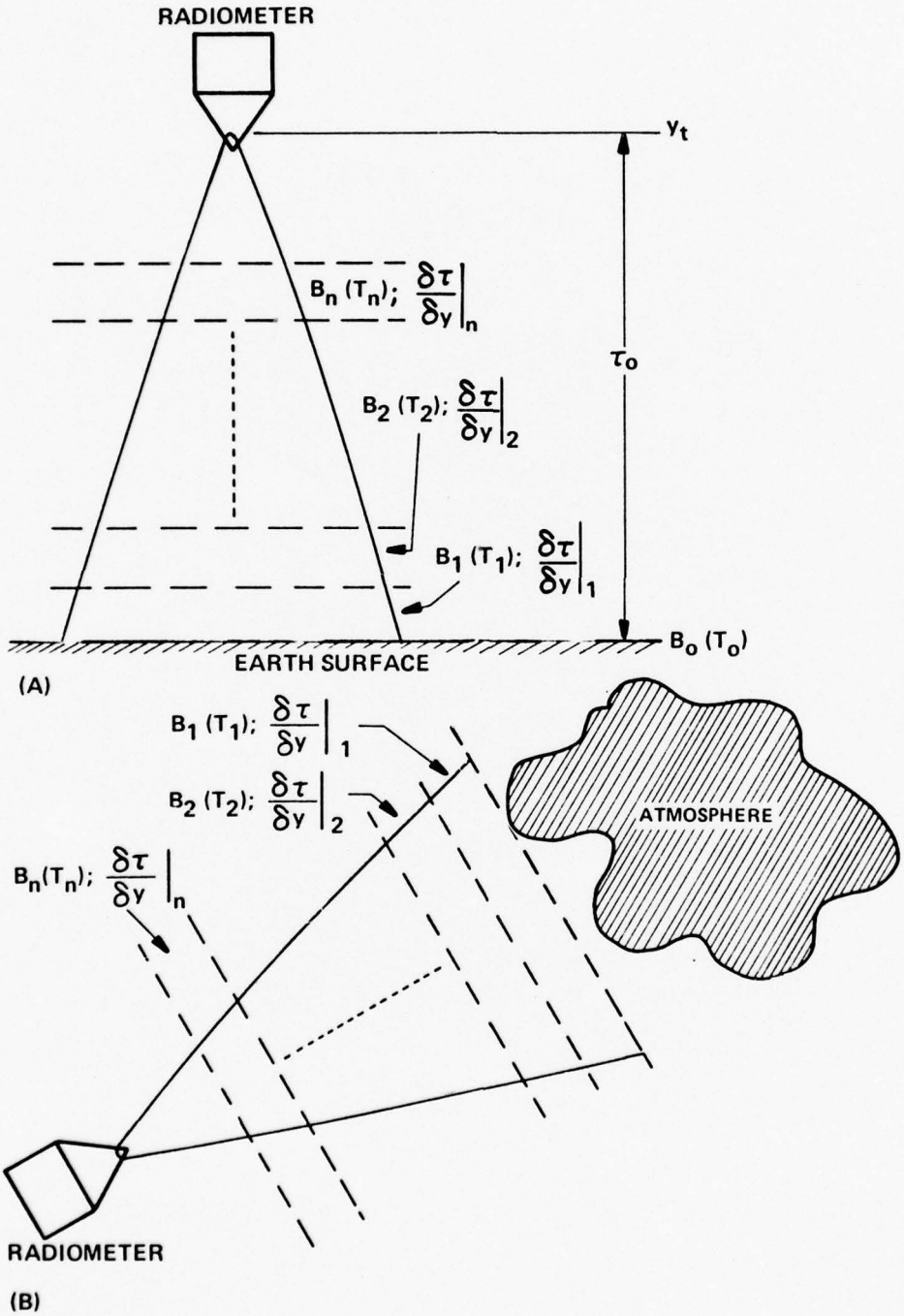

Figure 5. Behavior of Kernels (Weighting Functions) for Up-Looking and Down-Looking Systems

both quantities increase along the direction of radiation as shown in Figure 5B. Typical monochromatic weighting functions as a function of altitude are shown in Figure 6 for a down-looking system, and Figure 7 for an up-looking system. As may be seen from Figure 7, the spatial resolution for an up-looking radiometer is poor due to the exponential nature of the weighting functions.

IV. DIFFERENTIAL KERNEL APPROACH

In view of the above discussion it is clear that weighting functions generated in channels of an up-looking radiometer, which are solely based on spectral variations in the signature strengths of the active gases, suffer from inherently poor spatial selectivity. Hence, additional properties in the signature parameters must be utilized to generate selective kernel functions. A possible approach is the utilization of the inherently steep slope characteristics associated with the individual rotational emission lines of atmospheric gases as an additional degree of freedom. This requires sensing radiation from sections of a rotational emission line by means of a high spectral resolution radiometer.

Figure 8 illustrates a rotation line shape with Lorentzian attenuation profile which well represents pressure regions in the vicinity of ground levels of the atmosphere. The absorption as a function of wave number is given by:

$$\alpha(\nu) = \frac{S}{\pi} \quad \frac{\gamma}{(\nu-\nu_o)^2+\gamma^2} \qquad (9)$$

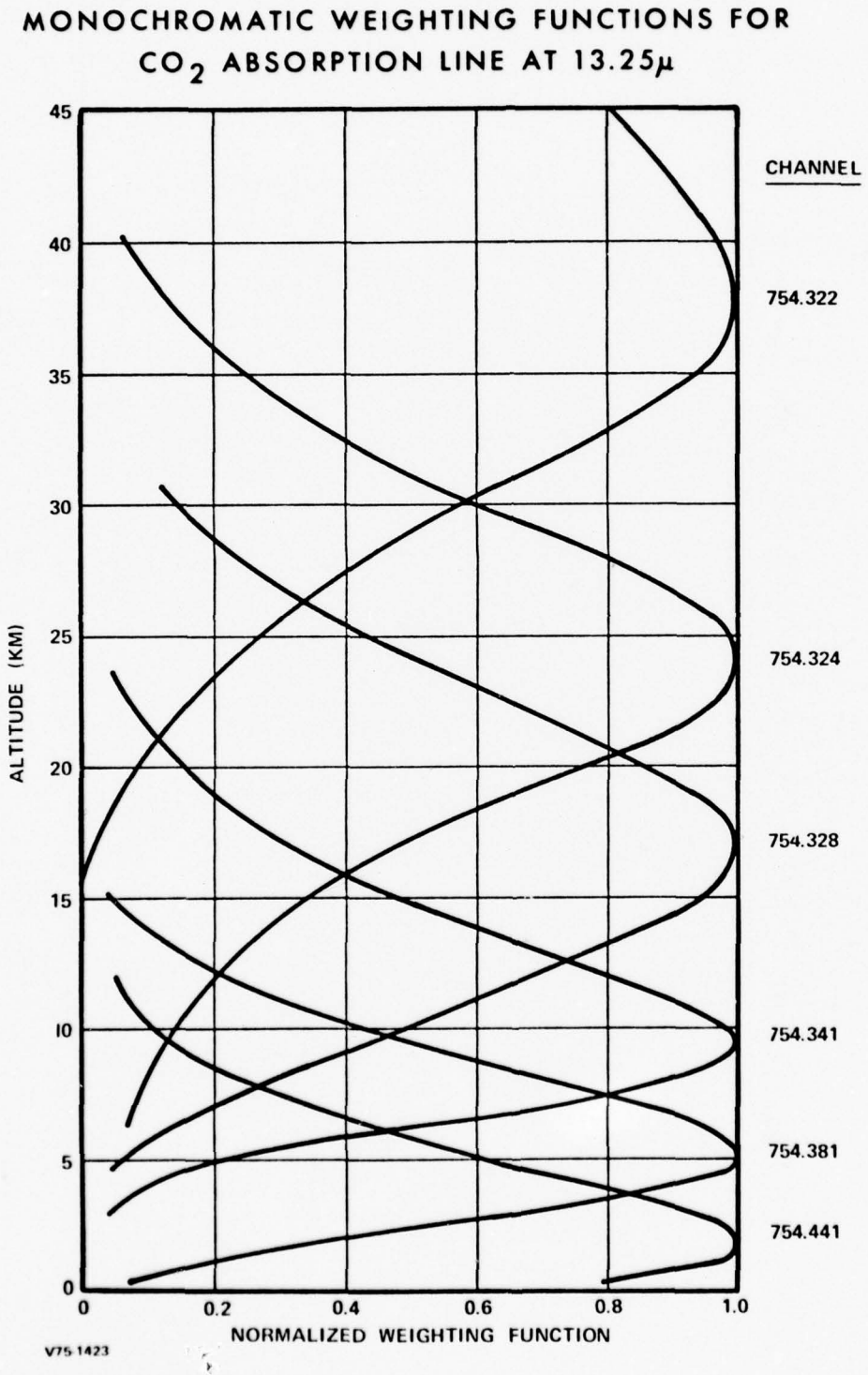

Figure 6. Monochromatic Weighting Functions for Down-Looking Radiometer

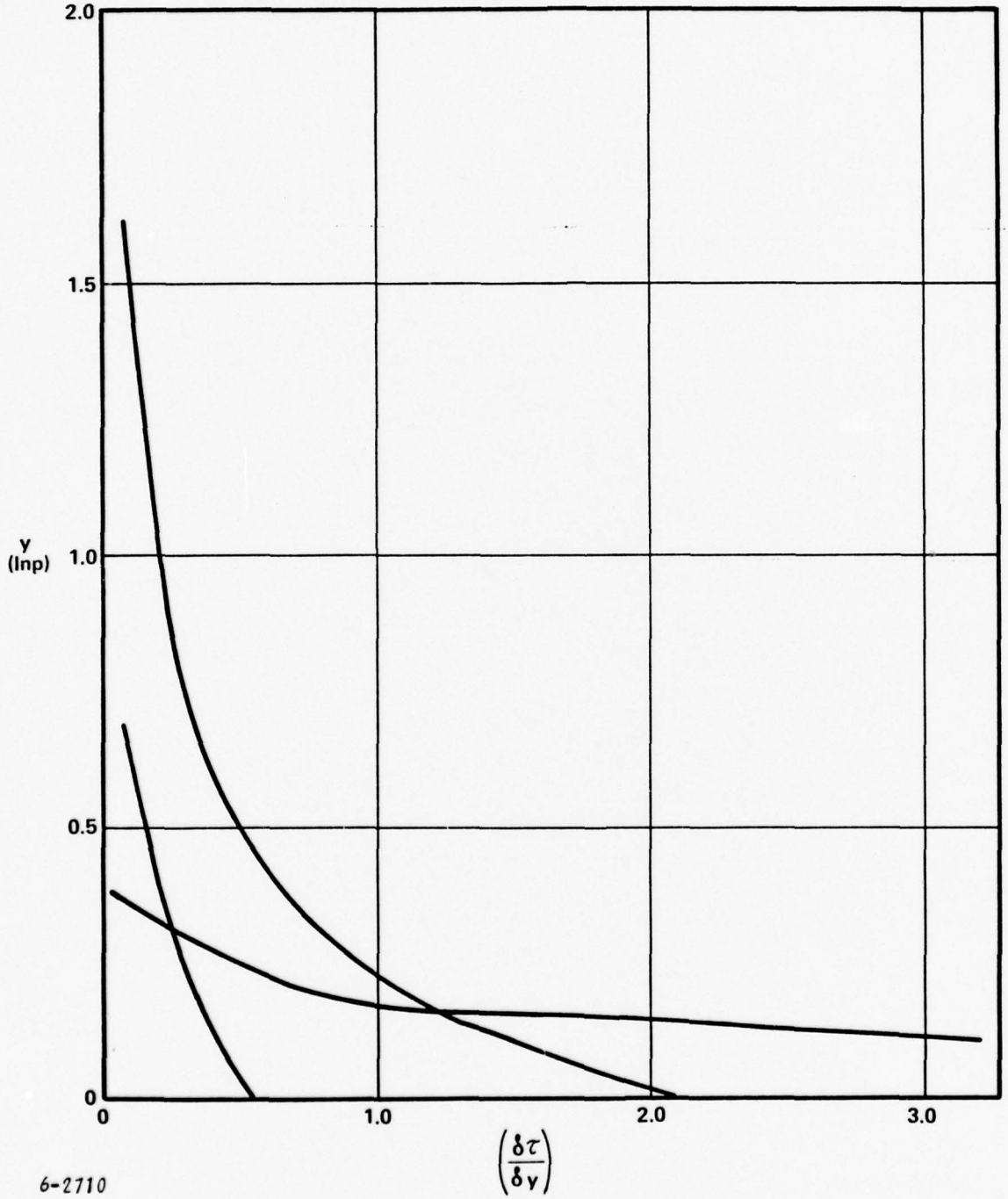

Figure 7. Monochromatic Weighting Functions for Up-Looking Radiometer

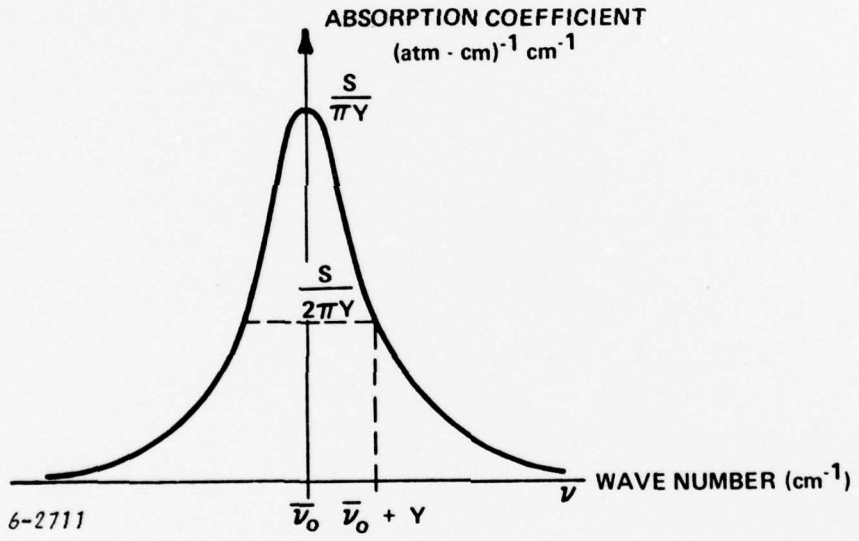

Figure 8. Lorentz Line Shape Profile

where

S = line intensity

γ = half-width at half maximum

ν, ν_o = variable and line center wave numbers, respectively

The altitude dependency of the absorption coefficient is due to the pressure variation in line width γ and is given by:

$$\gamma = \gamma_o p \tag{10}$$

where

$p = \frac{P}{P_o}$ = normalized pressure

P_o = pressure at ground level

γ_o = line width at ground level

The altitude (pressure) dependent transmission coefficient for monochromatic radiation (which is a good approximation for high resolution radiometers with channel spectral widths of the order or less than 1 percent of the absorption line width) is given by:

$$\tau(p) = \text{EXP}\left[-\int_{h_i}^{o} \alpha(p)\, w(p)\, \sec\theta\, dh\right] \tag{11}$$

and

$$w(p) = w_o p \tag{12}$$

where

$w(p)$ = gas concentration

w_o = concentration at ground level

$\alpha(p)$ = absorption coefficient

θ = zenith angle

h = altitude

Inserting equations (9), (10), and (12) into equation (11), and differentiating with respect to scale-height parameter y, the following expression for the weighting function is obtained:

$$\frac{\tau}{y} = \frac{k \sec \theta}{(1+C^2)^{k/2}} \quad \frac{p^2}{C^2+p^2} \quad \left[C^2+p^2\right]^{k/2} \tag{13}$$

where

$$\left.\begin{aligned} k &= \frac{Sw_o}{\pi \gamma_o} \\ C &= \frac{\nu-\nu_o}{\gamma_o} \end{aligned}\right\} \quad \text{Parameters independent of pressure}$$

$$p = e^{-y}; \left(y \approx \frac{h(km)}{7.5} = \text{pressure scale height}\right)$$

As an example consider the functional relationship of the weighting function with pressure for extreme spectral positions of sensor channels at two rotation lines of various signature intensities.

A. For the first channel located at line center:

$$C = 0$$

$$\frac{\partial \tau}{\partial y} \sim p^k \tag{14}$$

B. For the second channel located at the far wings of the line:

$$C >> p$$

$$\frac{\partial \tau}{\partial y} \sim p^2 \tag{15}$$

The difference-kernel generated from the absorption lines with corresponding channel positions (equations 11 and 12) is given by:

$$\left.\frac{\partial \tau}{\partial y}\right|_1 - \left.\frac{\partial \tau}{\partial y}\right|_2 = Ap^k - Bp^2 \qquad (16)$$

with a peak occurring at pressure level altitudes:

$$P_{peak} = \left[\frac{2}{k}\,\frac{B}{A}\right]^{\frac{1}{k-2}} \qquad (17)$$

where:

$$A = \frac{k \sec \theta}{(1+C^2)^{k/2}}$$

$$B = \frac{k_1 \sec \theta}{(1+C_1^{\,2})^{k_1/2}}$$

Thus peaked weighting functions may be generated from difference signals at two spectral line positions, with a spatial selectivity being a function of the radiative signature intensities of the two lines. It should be pointed out, however, that the difference kernel obtained from channels at extreme spectral positions are rather broad due to the shallow gradient at the far wing of the line and hence are inadequate for profiling the boundary layer with the required high spectral resolution.

Referring to Figure 8, it may be observed that a steep slope in the absorption line occurs in the vicinity of its half intensity position and hence its sensitivity to pressure variation will be large in this region. This suggests that narrower response difference kernels may be generated for channel positions in the vicinity of its steepest slope. This configuration is shown in Figure 9.

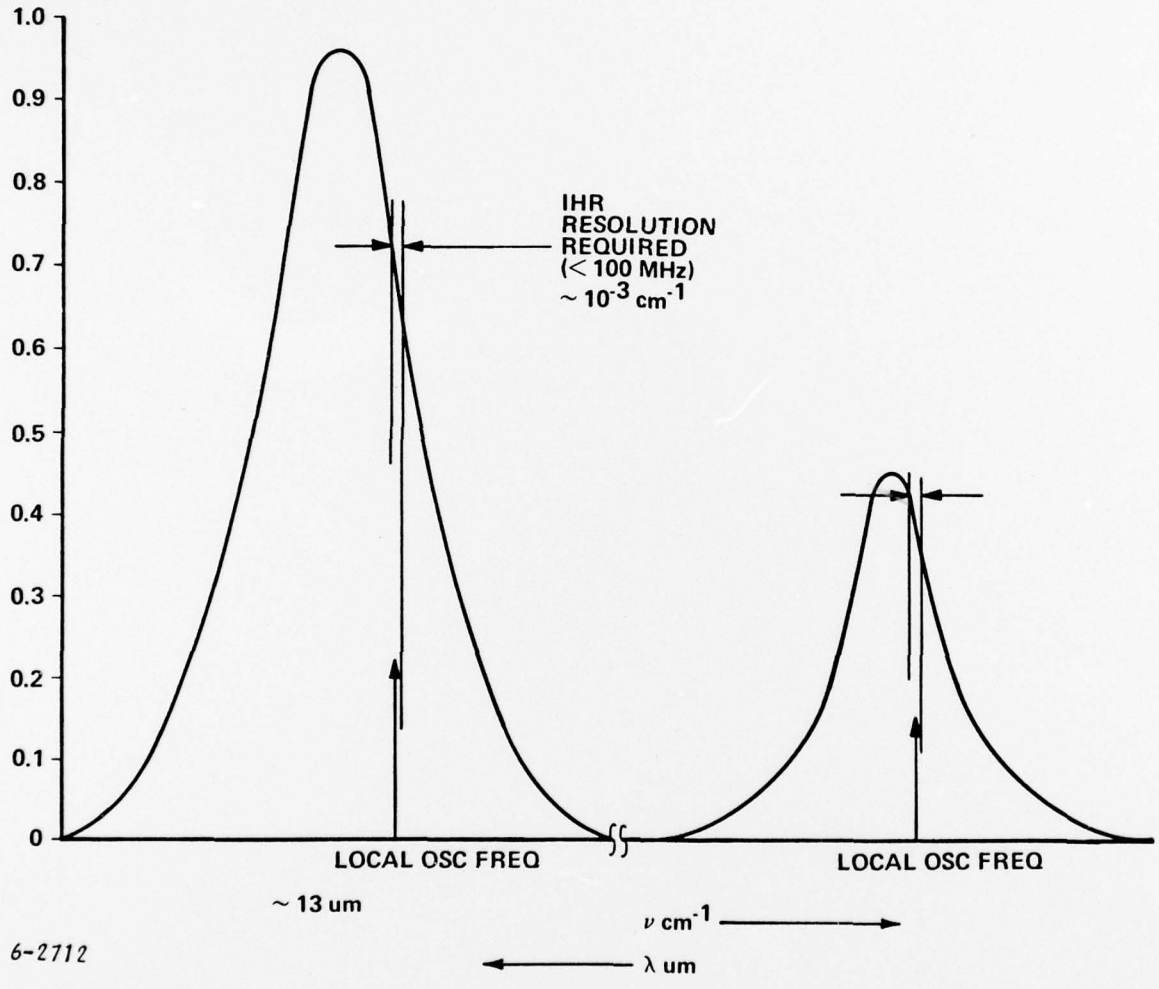

Figure 9. Schematic 2-Channel Arrangement for Generating Difference Kernels

V. GENERATION OF DIFFERENCE KERNEL FUNCTIONS

The CO_2 emission band at 13 μm was considered for generating differential kernel functions due to its high signature intensity characteristics and the feasibility of high spectral resolution instrumentation in the band (e.g., heterodyne radiometric techniques using tunable diode laser local oscillators). The technique however can be adapted at other spectral bands in the infrared or millimeter waves where discrete signature spectra due to uniformly mixed atmospheric gases exist.

The difference in kernels for two channels associated with two discrete lines, is given (see equation (13)) by:

$$\Delta = \left(\frac{\partial \tau}{y}\right)_1 - \left(\frac{\partial \tau}{y}\right)_2 = \sec\theta \left\{ K_1 \left[\frac{C_1^2 + \rho^2}{1+C_1^2}\right]^{K_1/2} \frac{\rho^2}{C_1^2+\rho^2} - K_2 \left[\frac{C_2^2 + \rho^2}{1+C_2^2}\right]^{K_2/2} \frac{\rho^2}{C_2^2+\rho^2} \right\} \tag{18}$$

where:

K_1, K_2 relate to signature strength of the two lines as defined in equation (13)

C_1, C_2 are normalized spectral positions of the two line channels

Thus, given two spectral lines of signature strengths K_1 and K_2, the spectral positions of the channels C_1 and C_2 which result in peaking the difference kernel at a given altitude, are found by minimizing equation (18) at a pressure P_1 corresponding to the altitude level, namely:

$$\frac{\partial \Delta}{\partial P}\bigg|_{P = P_1} = 0 \tag{19}$$

and solving for C_1 and C_2. Such computations were performed by solving the transcendental equation (18) for various combinations of line pairs and channel spectral positions, so as to obtain highly selective and contiguous difference kernel channels at the lower atmospheric levels.

Figures 10 and 11 show difference-weighting functions obtained for vertical, and 30-degree grazing-angle up-looking systems, respectively. As shown, narrow-width difference kernels result at contiguous regions immediately above ground level. The dotted lines shown in the figures represent undesirable reversal in sign (foldovers) in the difference functions which must be dealt with in the retrieval analysis so as to minimize this potential error. A simulated temperature retrieval based on the difference kernel was carried out and is discussed in Section IV.

VI. COMPUTER SIMULATED RETRIEVAL OF SUPERADIABATIC TEMPERATURE PROFILE

Retrievals of a typical superadiabatic lapse temperature profile were computer simulated using the three lower difference-kernel information channels in Figure 11. The algorithm adapted is based on iterative solutions of the radiative transfer equations and require no apriori statistical knowledge on atmospheric parameters. The method is based on the up-welling radiation retrieval proposed by W.L. Smith (Reference 5) which was modified here for a down-welling situation. The basic outline of the iterative computation procedure is as follows.

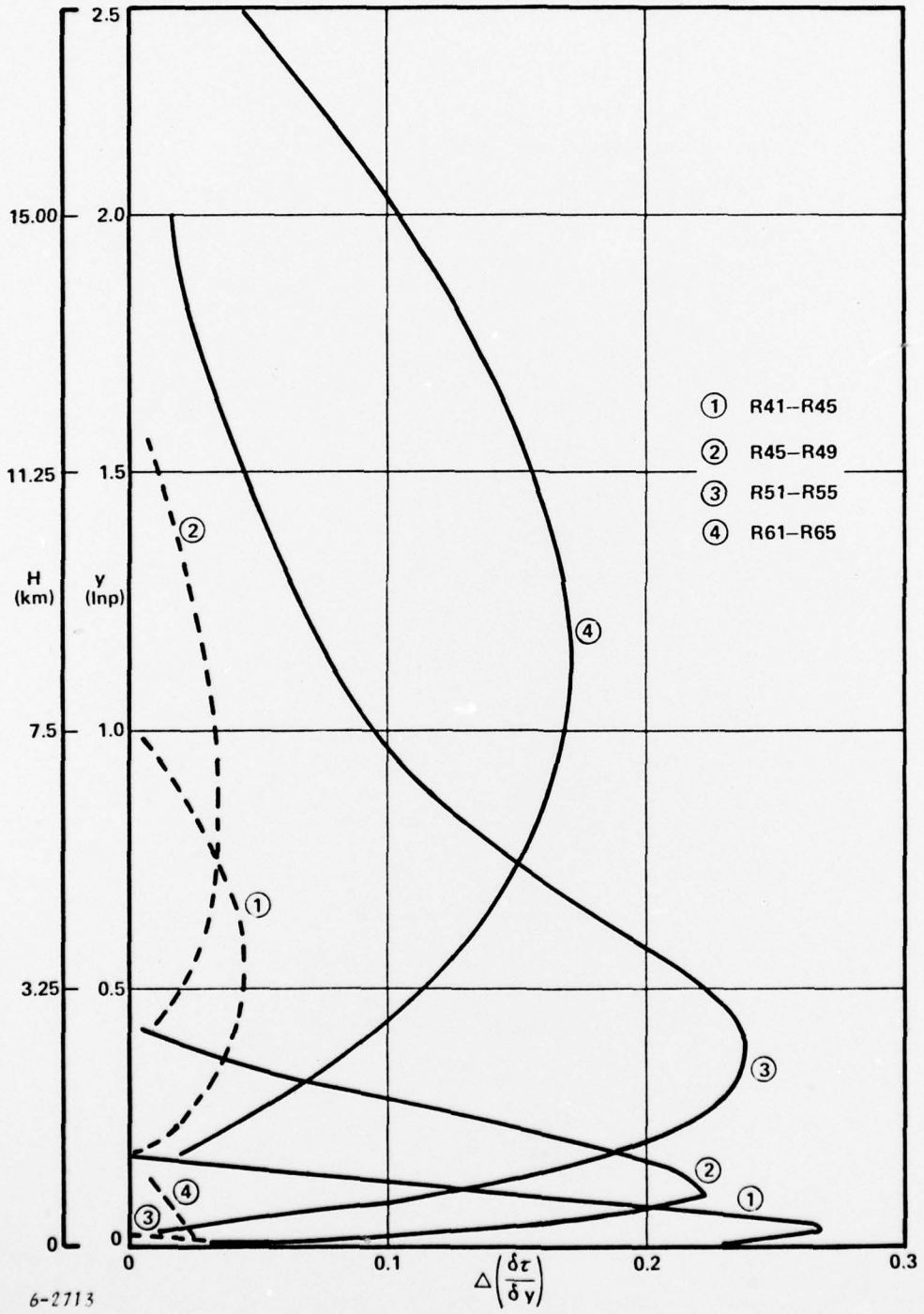

Figure 10. Differential Weighting Functions for Vertical Up-Looking System

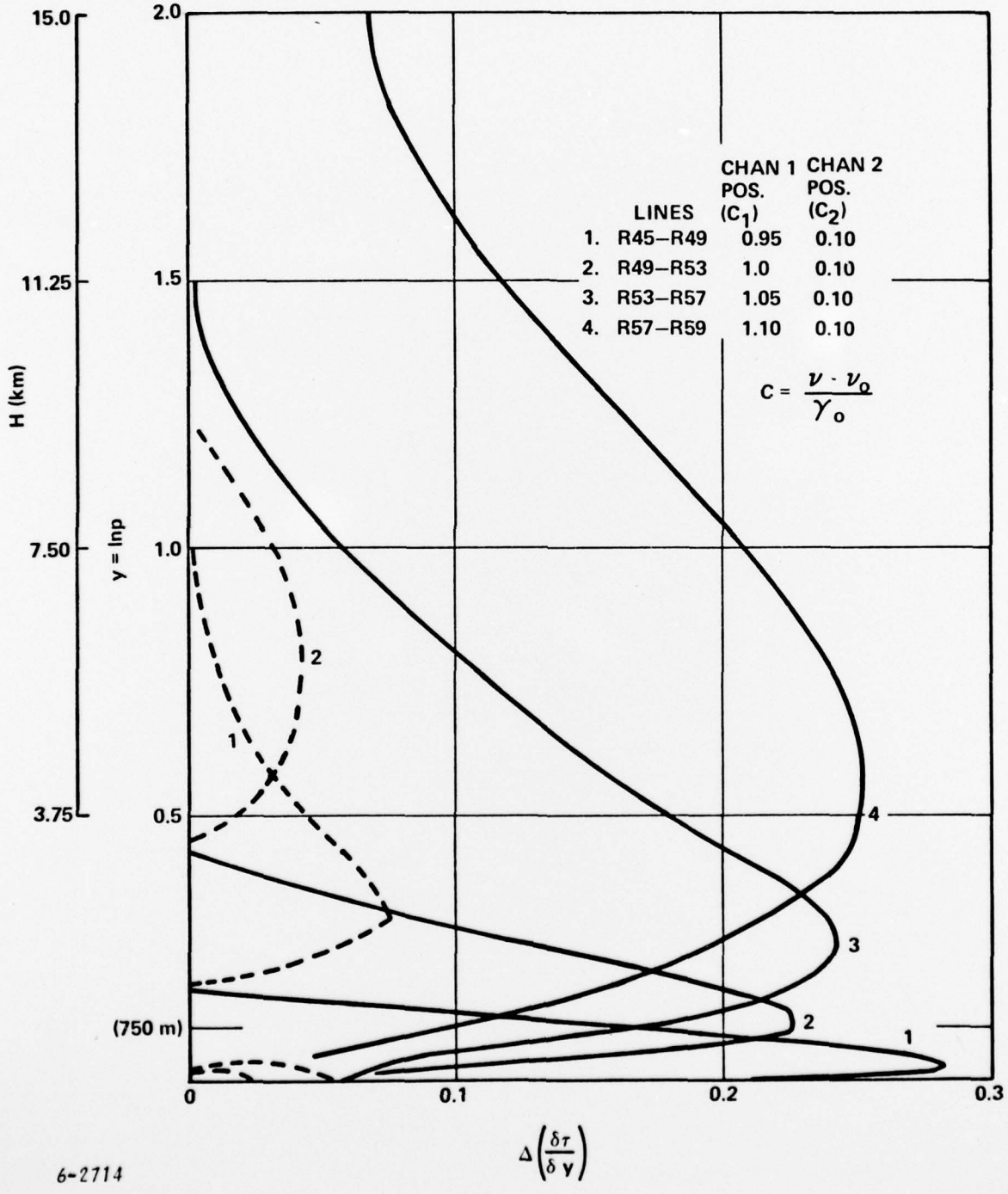

Figure 11. Differential Weighting Functions for 30-Degree Grazing-Angle Up-Looking System

A temperature altitude profile is first assumed, and designated as the "true" model atmosphere. The radiance corresponding to the "true" profile at each spectral channel is then computed from equation (5) by the method of digitization of the atmosphere in discrete isobaric incremental regions. The computed radiance levels at the channels are designated as the "measured" values. An arbitrary temperature profile designated as a "guessed" model is then assumed serving as a starting point in the iterative computational process. The radiances corresponding to the "guessed" model for all spectral channels as well as radiance ratios of "measured" to "guessed" values are initially computed.

As a first step in the iteration, "guessed" model radiances corresponding to each incremental altitude layer are updated in direct proportion to the computed radiance ratios of "measured" to "guessed" values. A first iterated model is then generated by averaging the temperatures corresponding to radiances of the spectral channels, each weighted by their characteristic kernel function at the given altitude. A relaxation method of iteration is adapted whereby spectral radiances at incremental atmospheric layers are continuously updated, proportionately to the ratio of the "measured" to computed values. New consecutive models are generated, based on averaged weighted temperature parameters from differential kernel functions at the given altitudes. The process continues until the difference between "measured" and computed spectral radiances are below a predetermined threshold value.

A simulated temperature retrieval for an assumed double inverted temperature profile, based on three information channels (Channels 1, 2, and 3 in Figure 11) is given in Figure 12. Curve A in the figure is the assumed "true" atmospheric profile, the dashed curve is the arbitrary assumed initial model in the iteration, and the retrieved model profile is as shown in curve C.

The two inversions in the assumed model at 374 m and 750 m altitude are reproduced in the retrieval. However, the fidelity of the retrieved profile in the lower 375 meters above ground level was insufficiently inaccurate due to excessive spatial widths in the kernel functions of the three channels. A more accurate temperature retrieval implementing four information channels with narrower spatial functions will be investigated during the next phase of the program.

VII. INFRARED HIGH SPECTRAL RESOLUTION RADIOMETRY

The required high spectral resolution of 10^{-3} to 10^{-4} cm^{-1} for sensing radiation from portions of a rotational emission line necessitates the utilization of state-of-the-art spectrometer techniques. Present day conventional spectrometers do not provide the required resolution. However, a heterodyne approach may be employed wherein a tunable laser (diode local oscillator) illuminates a photodiode simultaneously with the incoming source irradiance. The resulting IF signal is a high spectral resolution slice of the infrared radiation. This technique has been successfully employed in a number of equipment and instrumentation developments (References 2 and 3).

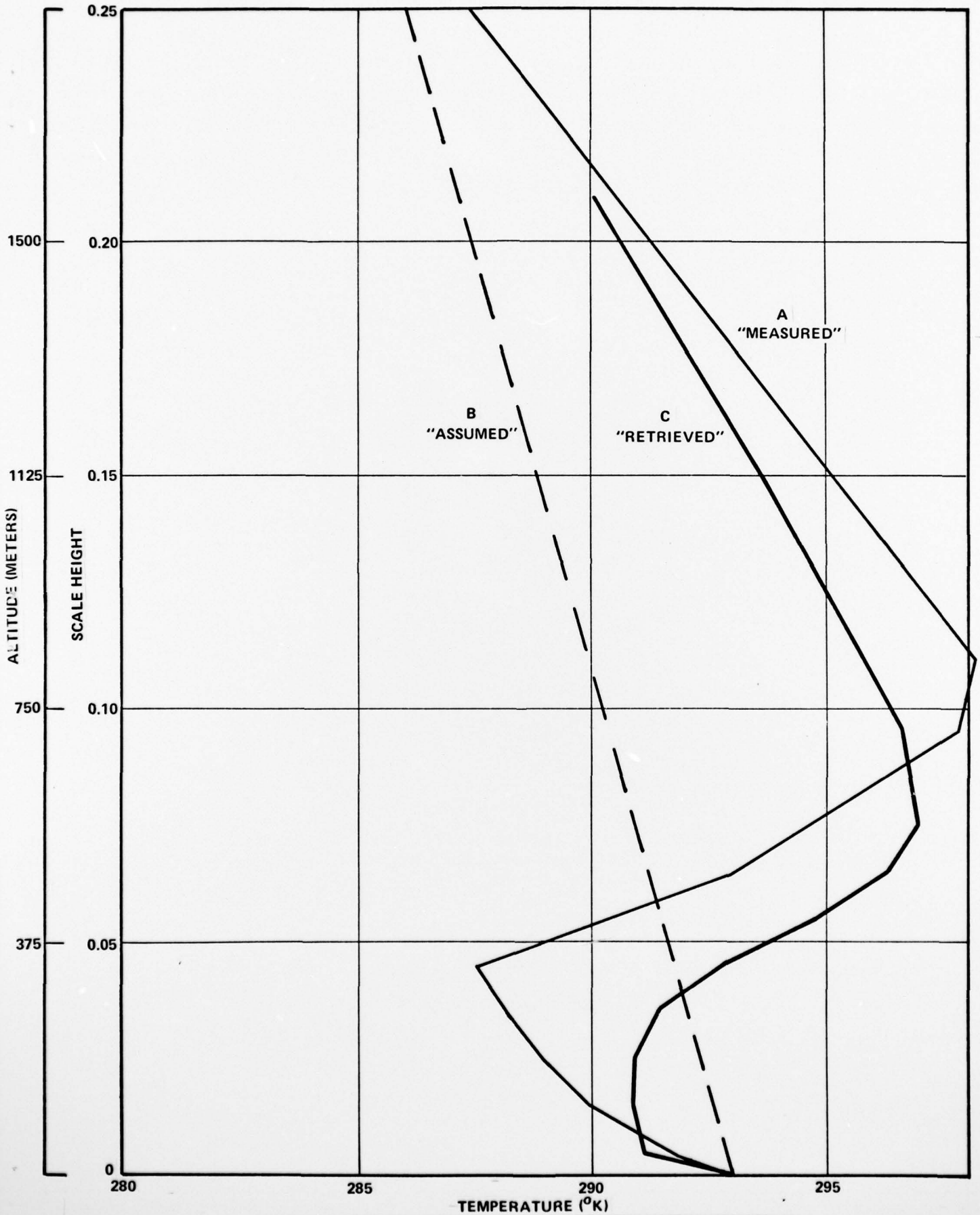

Figure 12. Computer Simulated Retrieval (3-Information Channels).

A dual-channel infrared heterodyne radiometer (IHR), as shown in Figure 13 (Reference 6), is currently being used to assess the concentration and vertical distribution of atmospheric ozone and ammonia by observing the up-welling radiance from different parts of the selected gas constituent line. The heterodyne radiometer techniques employed to measure gas concentrations can also be used to retrieve the thermal profile.

VIII. SUMMARY

A new method of remote profiling temperature and humidity gradients in the lower atmosphere by means of up-looking grazing-angle radiometer has been investigated. The technique consists of generating difference-kernel functions in several high spectral resolution channels. These functions are shown to have inherent high spatial resolution in the lower regions of the atmosphere. The results of a simulated retrieval of temperature profile with an assumed double inversion below an altitude of 1 km, based on three information channels, is presented.

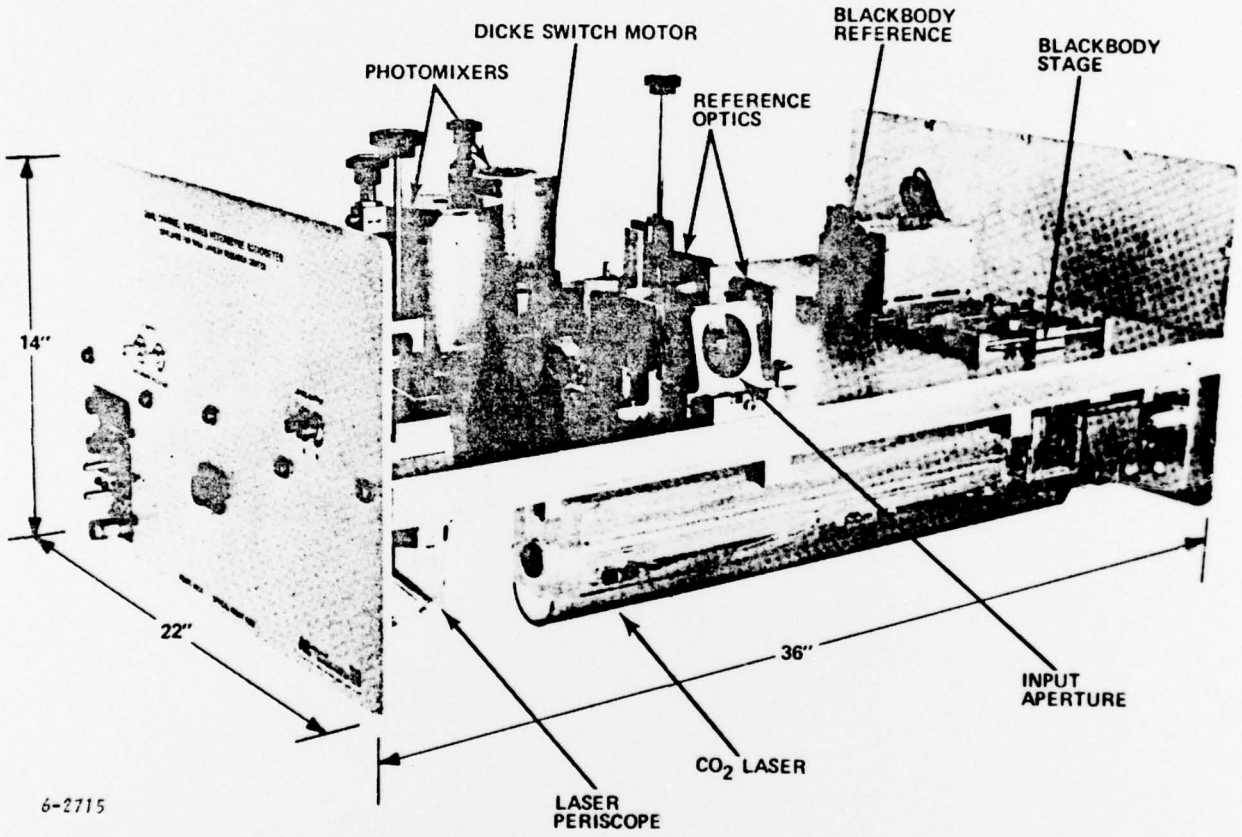

Figure 13. Infrared Heterodyne Radiometer

IX. REFERENCES

1. J.W. Walters, K.F. Kunzi, R.L. Pettyjohn, R.K.L. Poon and D.H. Staelin, "Remote Sensing of Altitude Temperature Profiles With the Nimbus 5 Microwave Spectrometer," Journal of Atmospheric Sciences, Vol. 32, pp 1953-1969, Oct. 1975.
2. B.J. Peyton, "Atmospheric Monitoring Using Infrared Heterodyne Radiometry," Proc. Int. Telemetering Conf., Los Angeles, Ca., Oct. 1974.
3. R.K. Seals and B.J. Peyton, "Remote Sensing of Atmospheric Pollutant Gases Using an Infrared Heterodyne Spectrometer," Proceedings of the International Conference on Environmental Sensing and Assessment, Vol. 1, p 10-4, Las Vegas, Nevada, Sept. 1975.
4. The U.S. Standard Atmosphere, Washington, D.C. U.S. Government Printing Office, 1962.
5. W.L. Smith, "Iterative Solution of the Radiative Transfer Equation for the Temperature and Absorbing Gas Profile of an Atmosphere", Applied Optics, Vol. 9, No. 9, Sept. 1970.
6. B.J. Peyton, et al, "Infrared Heterodyne Spectrometer Measurements of the Vertical Profile of Tropospheric Ammonia and Ozone," AIAA Conference, Los Angeles, Ca., Jan. 1977.